Protein Engineering, Design & Selection vol. 21 no. 6 pp. 405–412, 2008
Published online April 23, 2008 doi:10.1093/protein/gzn019

Balancing the stability and the catalytic specificities of OP hydrolases with enhanced V-agent activities

T.E. Reeves[1,2], M.E. Wales[1], J.K. Grimsley[1], P. Li[1], D.M. Cerasoli[2] and J.R. Wild[1,3]

[1]Department of Biochemistry and Biophysics, TAMU 2128, Texas A&M University, College Station, TX 77843-2128 and [2]Physiology and Immunology Branch, Research Division, United States Army Medical Research Institute of Chemical Defense, Aberdeen Proving Grounds, MD 21010-5400, USA

[3]To whom correspondence should be addressed.
E-mail: j-wild@tamu.edu

Rational site-directed mutagenesis and biophysical analyses have been used to explore the thermodynamic stability and catalytic capabilities of organophosphorus hydrolase (OPH) and its genetically modified variants. There are clear trade-offs in the stability of modifications that enhance catalytic activities. For example, the H254R/H257L variant has higher turnover numbers for the chemical warfare agents VX (144 versus 14 s^{-1} for the native enzyme (wild type) and VR (Russian VX, 465 versus 12 s^{-1} for wild type). These increases are accompanied by a loss in stability in which the total Gibb's free energy for unfolding (ΔG_{H_2O}) is 19.6 *k*cal/mol, which is 5.7 *k*cal/mol less than that of the wild-type enzyme. X-ray crystallographic studies support biophysical data that suggest amino acid residues near the active site contribute to the chemical and thermal stability through hydrophobic and cation–π interactions. The cation–π interactions appear to contribute an additional 7 *k*cal/mol to the overall global stability of the enzyme. Using rational design, it has been possible to make amino acid changes in this region that restored the stability, yet maintained effective V-agent activities, with turnover numbers of 68 and 36 s^{-1} for VX and VR, respectively. This study describes the first rationally designed, stability/activity balance for an OPH enzyme with a legitimate V-agent activity, and its crystal structure.

Keywords: cation–π interactions/chemical warfare agents/organophosphorus hydrolase/protein stability/rational design

Introduction

Some of the most neurotoxic chemical warfare agents (CWAs) are organophosphate (OP) G- and V- agents, which irreversibly bind to acetylcholinesterase and cause cholinergic paralysis (Dacre, 1984; Gallo and Lawryk, 1991). The extensive search for detoxifying enzymes that can counteract these effects has led to attempts to train abzymes to hydrolyze neurotoxins (Grognet *et al*., 1993; Yx *et al*., 1995), redirect cholinesterase activities (Masson, 1998; Millard, 1998), and form select hydrolytic enzymes by directed evolution (Yang *et al*., 2003; Roodveldt and Tawfik, 2005). In the current studies, the nature of a very active V-agent hydrolyzing enzyme, derived from organophosphorus hydrolase (OPH), is reported.

OP hydrolases are a relatively small group of enzymes (EC 3.1.8) capable of hydrolyzing a wide spectrum of OP neurotoxic pesticides and CWAs (Mazur, 1947; Garden *et al*., 1975; Mulbry *et al*., 1986; McDaniel *et al*., 1988; Adkins *et al*., 1991; Cheng *et al*., 1996). The most characterized enzyme is the organophosphorus hydrolase (OPH, EC 3.1.8.1) from *Brevundimonas diminuta* (previously *Pseudomonas diminuta*). The protein is a distorted homodimer that folds as an $(\alpha\beta)_8$-barrel. A catalytic water or an activated hydroxyl group bridges the two active site, divalent cation metals in each monomer. The activated water hydrolyzes substrates via a S_N2 reaction (Lewis *et al*., 1988; Aubert *et al*., 2004), which includes a wide variety of OP compounds containing phosphotriester (P–O), phosphonothioate (P–S), phosphonofluoridate (P–F) and phosphonocyanate (P–CN) bonds. While the enzyme's natural substrate and function remain unknown, it is most effective at hydrolyzing the P–O bond of the phosphotriester insecticide paraoxon, which has catalytic rates approaching the limits of diffusion (10^8–10^9 M^{-1} s^{-1}). The activity of native OPH varies between the different phosphonothioate substrates, exhibiting a more limited efficacy against the P–S bond of demeton-S ($k_{cat} = 4$ s^{-1}) (Lai *et al*., 1995; Kolakowski *et al*., 1997; diSioudi *et al*., 1999a). The CWAs VX (O-ethyl S-diisopropyl aminomethyl methylphosphonothioate) and VR (*O*-isobutyl *S*-N,N-diethylaminoethyl methylphosphonothioate) belong to this class of modestly hydrolyzed compounds (P–S bonds) (Lai *et al*., 1995; Kolakowski *et al*, 1997; Rastogi *et al*., 1997). Thus, the rational design of OPH to enhance its degradation of these phosphonothioate nerve agents was of interest.

Previous research efforts have focused on improving the catalytic efficiency and substrate specificity of OPH variants directed toward the various classes of neurotoxic pesticides and CWAs. In initial mutational studies of the native OPH, the histidines at positions 254 and 257 were replaced, creating variants with increased activity and enhanced specificity for the phosphonothioate (P–S) substrates (Lai *et al*., 1996; diSioudi *et al*., 1999b). Recent random directed evolution studies have supported the importance of residues 254 and 257 in the hydrolysis of these toxic compounds, which include the CW V-agents and the G-agents (Hill *et al*., 2003). In addition, the enzyme's affinities for isomeric forms of P–F substrates have been altered to make them more efficient at degrading analogs for the most toxic isomers of GD (soman) (Chen-Goodspeed *et al*., 2001a,b; Hong *et al*., 2004). These and various other substrate-efficiency studies have demonstrated that it is possible to tailor the enzyme's catalytic properties; however, few studies have addressed the effects of substitutions in and near the active site on the stability of the enzyme.

While OPH can functionally accommodate many different metals, the Zn^{2+} form of OPH is one of the most stable dimeric proteins ever identified, with a conformational stability of 40 *k*cal/mol. The Co^{2+} form is the most active of the

metal-liganded forms. The Zn^{2+} form of the enzyme unfolds via a three-state pathway, such that the active, native folded dimer (N_2) transitions to a partially unfolded, inactive dimeric intermediate (I_2), and then to the unfolded monomers (2U), $N_2 \rightarrow I_2 \rightarrow 2U$ (Grimsley *et al.*, 1997). The dimeric interface contributes 36–38 *k*cal/mol of the total 40 *k*cal/mol in thermodynamic stability (Grimsley *et al.*, 1997). A loss of activity prior to the transition from the native dimer to the intermediate, $N_2 \rightarrow I_2$, suggests that the active site, or regions closely linked to the active site, denature during this phase of the unfolding pathway.

Evaluation of the available crystal structures of OPH revealed a stacking network within the three-dimensional orientation of residues 254 and 257 (Fig. 1A) (Benning *et al.*, 1994; Grimsley *et al.*, 2005). In this study, the role of aromatic stacking, hydrophobic interactions, and cation–π interactions involving these residues in establishing the stability of the enzyme is considered. Fluorescence emission was used to follow changes in the global conformation of OPH. The selective excitation of tryptophan residues, and their close proximity to residues 254 and 257, has allowed the observation of local changes in the protein. The global and local unfolding information suggest a model for the initial unfolding of OPH. In total, this study provides insight into the integration of structure and function in OPH, and it has led to the design and construction of stable and active V-agent hydrolyzing enzymes.

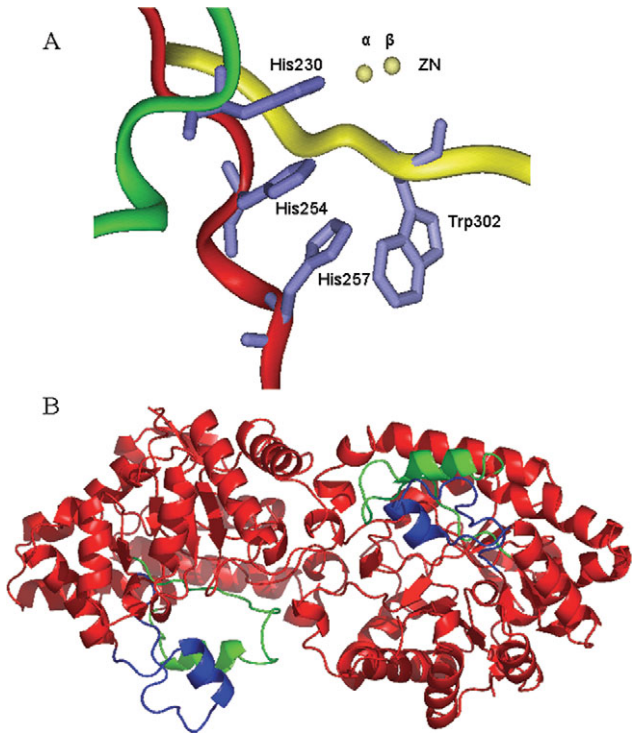

Fig. 1. Structural characteristics of OPH. (A) The active site metals of OPH and the stacking network consisting of H230, H254, H257 and W302. The green, red and yellow distinguish three secondary structural elements with residues involved in the stacking network. (B) Location of the stacking network in the OPH dimer. Helices adjacent to the active site, which are connected by residues 257 and 302, are depicted in green (residues 299–323) and blue (residues 253–276). Figures were created using PyMol Molecular Graphics System (2002) DeLano Scientific, San Carlos, CA, USA, and coordinates were utilized from the PDB file 1DPM (Benning *et al.* 1995).

Materials and methods

Variant enzyme construction and purification

The RH, RL, and HL variants were constructed as previously described (Lai *et al.*, 1996; diSioudi *et al.*, 1999b). Since cobalt confers the most enzymatic activity on the enzyme, only that form was used in this study. The two-character nomenclature refers to the amino acids at positions 254 and 257, i.e. the wild-type HH has a histidine at both the positions 254 and 257. The leucine at position 257 in the RL variant was subsequently replaced with a phenylalanine to generate the H254R/H257F (RF) variant using the QuikChange XL mutagenesis kit (Stratagene). Primers to construct the L257F mutation (5′-gcatcccgttcagtgcgattg gtctag-3′ and 5′-ctagaccaatcgcactgaacgggatg-3′) were synthesized by IDT Inc. The resulting mutants were verified by sequencing, and the plasmid was transformed into *Escherichia coli* DH5α for expression and purification. The enzymes were purified as previously described (Grimsley *et al.*, 1997) and concentrated to 1–10 mg/ml for storage up to six months at 4°C in the final column buffer (10 mM KPO_4, 20 mM KCl, 50 μM $CoCl_2$, pH 8.3). Protein concentration was determined using an extinction coefficient of 58 000 M^{-1} cm^{-1} when measuring absorbance at 280 nm. Purity was verified by SDS–PAGE (sodium dodecyl sulfate polyacrylamide gel electrophoresis).

Enzyme activity assays

Paraoxon and demeton-S were purchased from ChemService. The free thiol reporter for the demeton-S assays was 2,2′ dithiodipyridine (2,2′ TP) and DTNB (Ellman's reagent) for VX and VR. VX and VR in saline were provided to USAMRICD by ECBC (Edgewood Chemical Biological Center, Aberdeen Proving Ground, MD, USA), and assays were performed at the US Army Medical Research Institute of Chemical Defense (Aberdeen Proving Ground, MD, USA). Michaelis constants (K_M) and the catalytic rates (k_{cat}) for paraoxon and demeton-S were determined by performing enzymatic assays with varying concentrations of substrate and constant enzyme concentrations. The data were fit using Origin 7.0 software (Microcal).

Paraoxon hydrolysis was followed by measuring the appearance of the p-nitrophenol anion at 400 nm (ε = 17 000 M^{-1} cm^{-1}) in 20 mM CHES (pH 9.0) at 25°C, and initial velocities were calculated and fit to the Michaelis–Menten equation, allowing for substrate inhibition.

Demeton-S hydrolysis was followed by the appearance of the 2,2′ TP anion at 343 nm (ε = 7060 M^{-1} cm^{-1}) in tripart buffer (pH 8.0) (diSioudi *et al.*, 1999b). VX and VR hydrolysis was monitored by the appearance of the TNB anion at 405 nm (ε = 14 150 M^{-1} cm^{-1}) in 10 mM phosphate, 50 μM $CoCl_2$, 20 mM KCl, pH 8.3 and initial velocities were calculated and fit to the Michaelis–Menten equation. Due to limited V-agent availability, only those enzymes with the desired demeton-S profiles were tested with the OP nerve agents, VX and VR. Furthermore, saturation of the enzymes with V-agents was not possible because of concentration limitations established for research with neurotoxic surety materials at USAMRICD. The maximum concentration available was 2 mM; therefore turnover numbers were calculated at that concentration.

Chemical denaturation

Chemical denaturation experiments were performed as previously described (Grimsley *et al*., 1997). The final concentration of enzyme was 100 μg/ml for all denaturation experiments. Fluorescence samples were incubated for 24 h at 25°C in 0–4 M GdmCl or 0–8.5 M urea. Denaturants were prepared in 10 mM phosphate, 50 μM $CoCl_2$, 20 mM KCl buffer, pH 8.3 (Pace and Scholtz, 1997). Fluorescence data were collected on an AVIV 105ATF fluorometer using an excitation wavelength of 278 nm and an emission wavelength of 320 nm, where the maximum difference exists between the native and denatured state of the protein. The signal averaging time was 30 s at 25°C using 1 cm path length cuvettes. Fluorescence signals were normalized and data were analyzed as described previously (Grimsley *et al*., 1997).

8-Anilino-1-naphthalenesulfonic acid (ANS) has been shown to be a sensitive probe for partially folded intermediates in protein-folding pathways. ANS was added to enzyme samples from the chemical denaturation experiments to a final concentration of 50 μM and incubated for 1 h. The emission from ANS alone in aqueous solution has a maximum above 500 nm. In the presence of protein, however, the wavelength maximum is blue shifted to 470 nm, as a result of adsorption onto non-polar regions of the protein surface. ANS-protein samples were excited at 385 nm and the emission read at 470 nm in an AVIV 105ATF spectrofluorometer at a cell temperature of 25°C, with an averaging time of 30 s, using a 1 cm path.

Selective tryptophan fluorescence

To monitor local environments around tryptophan residues, fluorescent wave scans of the enzymes were collected with an AVIV 105ATF spectrofluorometer using an excitation wavelength of 295 nm and recording the emission between 310 and 450 nm at 25°C.

Thermal denaturation

Thermolysin digests were performed at 65°C and at an OPH:thermolysin mass ratio of 250:1 with 5 μM $CaCl_2$ in 10 mM Tris (pH 8.3). OPH was pre-incubated for 2 min at 65°C and control samples were removed. Thermolysin was added to the remaining reactions to initiate digestion and aliquots were removed at 1, 5 and 15 min and the digestion was stopped for each aliquot by the addition of SDS loading dye and boiling for 2 min. Proteolysis samples were then analyzed by SDS–PAGE. The relative band intensities between the control, 1, 5 and 15 min samples were determined using TotalLab v2005, and fit to Eq. (1) to estimate the half lives of the enzymes under these conditions, where t_0 is the band intensity of the control lanes. As with the tryptophan excitation experiments, the protein concentrations were determined using the extinction coefficient and the Bradford assay.

$$[A]_{t_{1/2}} = [A]_{t_0} e^{-kt} \quad (1)$$

Crystallization, structure determination and refinement

Immediately following purification, the RF variant was concentrated to 17 mg/ml, followed by repeated washes in crystallization buffer, 20 mM HEPES, pH 7.5. The concentrated enzyme was stored at 4°C and used within 24 h. The protein was diluted to 10 mg/ml with crystallization buffer. Single crystals were grown by the hanging drop method (McPherson, 1999) at room temperature. The crystallization solution contained 10% PEG6000, 0.1 M HEPES, pH 7.0, 1% EBP (diethyl 4-methylbenzylphosphonate), a substrate analog for demeton-S, and 5 mM sodium azide. No additional cobalt was added to the crystallization solution.

H254R/H257F crystals were serially transferred to cryoprotectant solutions of a synthetic mother-liquor containing 5–30% glycerol, and flash-frozen in liquid nitrogen. Diffraction data for the mutant crystal was collected using a RAXIS IV^{++} detector mounted on a Rigaku HF007 generator. All data were processed with the HKL2000 package (Otwinowsky and Minor, 1997). The structure of H254R/H257F was determined by difference Fourier using the H254R (PDB:1QW7; Grimsley *et al*., 2005) enzyme structure as the start model. Manual rebuilding was performed with the program O (Jones and Kjeldgaard, 1997) and refined in CNS (Brunger *et al*., 1998).

Identification of cation–π interactions

The CaPTURE program (Gallivan and Dougherty, 1999) (http://capture.caltech.edu/) was obtained from the Division of Chemistry and Chemical Engineering, California Institute of Technology, Pasadena, CA, USA, and used for identifying cation–π interactions. Three crystal structures were analyzed: (1) the zinc-liganded, wild-type OPH enzyme, pdb:1DPM; (2) the H254R enzyme, pdb:1QW7 and (3) the RF variant constructed in this study. This program makes it possible to partition the electrostatic and van der Waals components of the calculated cation–π interaction energy.

Results

Position 257 plays an important role in the stability of OPH

Genetically engineered variants of OPH were created by substituting the native histidines at positions 254 and 257 (Fig. 1A) to create a coordinated set of enzymes: HH (the native enzyme with histidine at both 254 and 257), HL (a variant with histidine at 254 and leucine at 257), RH, RL, and RF (variants with arginine at 254 and histidine, leucine or phenylalanine, respectively, at 257). The unfolding free energies (ΔG_{H_2O}) of HH, RL, and HL were determined from urea equilibrium denaturation data (Table I and Fig. 2). A comparison of the ΔG_{H_2O} values allows for an evaluation of each substitution's contribution to the global stability, and suggests that the substitution of a leucine at position 257 plays an important role in the decreased stability of these enzymes. The transition from the native state to the folded intermediate, $\Delta G^\circ 1$ and indicated as $N_2 \leftrightarrow I_2$ in the unfolding

Table I. Conformational stabilities in *k*cal/mol determined by equilibrium urea denaturation and monitored by intrinsic tryptophan fluorescence

Enzyme		$\Delta G^\circ 1$	$\Delta G^\circ 2$	$\Delta G^\circ H_2O$
HH	H254, H257	3.4 ± 1.3	21.9 ± 1.9	25.3 ± 3.2
RL	H254R, H257L	2.3 ± 0.6	17.3 ± 0.9	19.6 ± 1.5
HL	H254, H257L	0.9 ± 1.0	19.4 ± 1.0	20.3 ± 2.0

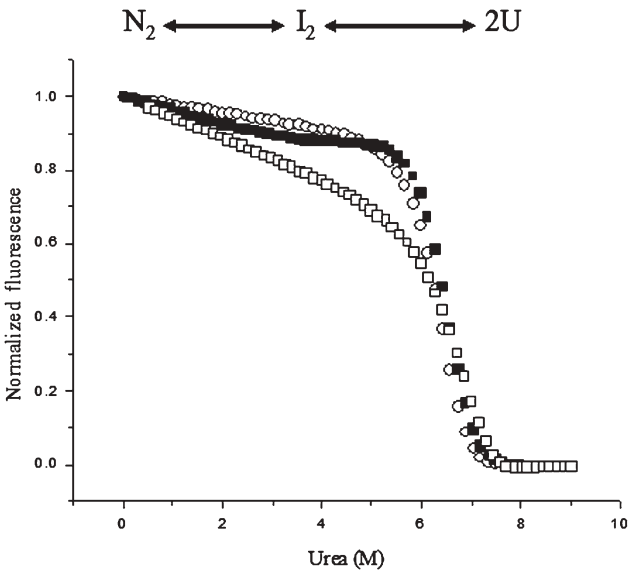

Fig. 2. Urea denaturation of OPH enzymes. HH (■), HL (□) and RL (○). Protein concentrations were 100 μg/ml. Fluorescence was monitored by excitation at 278 nm and emission recorded at 320 nm. Normalized curves were fit using an equation describing a three-state unfolding model. The RH and RF enzymes were not completely denatured up to 8 M urea and are not shown; therefore, the conformational stabilities for these two enzymes could not be determined using urea.

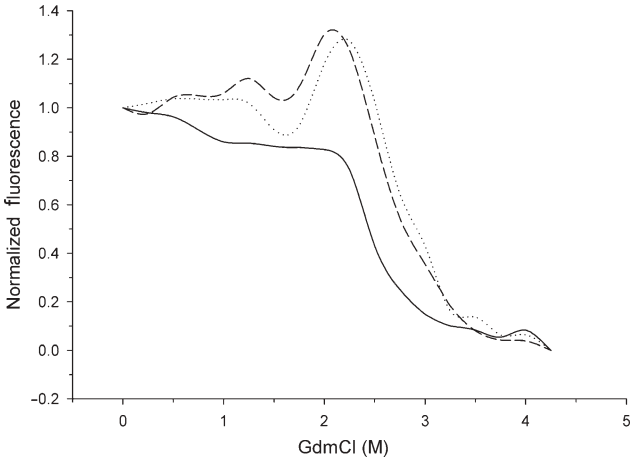

Fig. 3. GdmCl denaturation of OPH enzymes. RH (dotted line), RF (dashed line) and HH (solid line). Protein concentrations were 100 μg/ml. Fluorescence was monitored by excitation at 278 nm and emission recorded at 320 nm. Normalized curves for RH and RF could not be fit to an unfolding model due to multiple inflections in the region between 1 and 2.5 M GdmCl. The RH and RF variants display a local minimum at 1.5 M GdmCl.

pathway, was variable among the HH, RL, and HL family of enzymes, while the transition from the folded intermediate to the unfolded monomers, $\Delta G^{\circ}2$ and indicated as $I_2 \leftrightarrow 2U$, was more uniform (Fig. 2 and Table I). This is an important distinction, as the first transition has been shown to result in an inactive intermediate (Grimsley *et al*., 1997), thus demonstrating that the decreases in the ΔG_{H_2O} are associated with structural changes in the active site sufficient to alter activity.

Alternatively, retaining the native histidine at 257 in the RH variant resulted in an enzyme, which was not completely denatured by urea concentrations up to 8.5 M, even after incubation for 24 h. For this reason then, RH and HH were compared when GdmCl was used as the denaturant. Under these conditions, RH exhibited two inflections in the intrinsic fluorescence trace which precluded determination of ΔG_{H_2O}; however, the curve was shifted slightly to higher GdmCl concentrations than for HH (Fig. 3). This suggests that the RH variant was a more stable enzyme than the HH (or either of the 257L enzymes). These results are consistent with the activity analysis, which demonstrated that the RH enzyme retained residual activity above 2 M GdmCl and 8 M urea. In summary, because of the complex denaturation profile with GdmCl and incomplete denaturation with urea, the Gibb's free energies of folding for the RH variant could not be determined by chemical denaturation.

Design and characterization of more stable OP hydrolyzing enzymes

Variants with an arginine at position 254 have a 10–12-fold increase in activity with P–S substrates (Lai *et al*., 1996; diSioudi *et al*., 1999a). Evaluation of the HH crystal structure revealed that the orientation of 257 with 302 creates an edge-to-face stacking interaction (Fig. 1A) (Benning *et al*., 1994). The RL and HL variants, which disrupt this interaction, are less stable enzymes (Table I). It was hypothesized that engineering a substitution at position 257 to provide a stronger interaction with 302 may result in a more stable enzyme; while combining this with an arginine at position 254 should confer the desired enhancement of P–S activity. To test this hypothesis, the H254R/H257F variant was produced.

Similar to the RH enzyme, the GdmCl denaturation curves of the RF variant (Fig. 3) displayed the same complex spectra while the enzyme was incompletely denatured at 8 M urea. Since the ΔG_{H_2O} of these variants could not be determined by chemical denaturation, limited proteolysis during temperature denaturation was used to evaluate the relative stabilities.

The paradigm supporting the use of proteolysis for this purpose is that compact or folded structures have fewer accessible proteolysis sites, and are thus more resistant to digestion (Arnold and Ulbrich-Hofmann, 2001). The susceptibility of each variant to thermal denaturation was followed by thermolysin digests after 1, 5 and 15 min at 65°C (Fig. 4B). The RH and RF variants were the most resistant to proteolysis, while the HL and RL variants were significantly degraded after 5 min. The relative stabilities of the variants can be ordered as follows: RL < HL < HH < RH < RF with $t_{1/2}$ values at 65°C estimated to be ~1.3, 1.8, 2.2, 4.3 and 11 min, respectively. This is consistent with the relative stability of those enzymes for which the ΔG_{H_2O} could be determined (Table I).

Probing the initial steps in unfolding

Positions 254 and 257 are in close proximity to W302 (Fig. 1), thus making tryptophan excitation a valuable tool for examining local changes in the tertiary structure. Selective excitation of the tryptophan residues revealed significant differences in the maximal emissions among the enzymes, suggesting the local environments of the tryptophans are dissimilar (Fig. 5). The enzymes with the strongest tryptophan emissions were the HH and HL. The introduction of an arginine at position 254 in the RL and RH enzymes resulted in quenching of tryptophan emission. Further

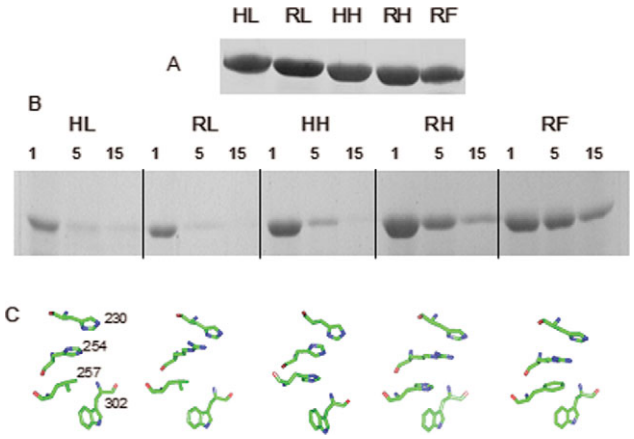

Fig. 4. Thermal denaturation of OPH enzymes using limited proteolysis with thermolysin. Protein concentration was 1 mg/ml and the OPH:thermolysin mass ratio was 250:1. (A) Zero time control, enzymes prior to digestion. (B) Thermolysin resistance of enzymes at 65°C. The digestions were stopped at 1, 5 and 15 min intervals by boiling each sample for 2 min in SDS loading buffer. The estimated $t_{1/2}$ values for HL, RL, HH, RH and RF were 1.8, 1.3, 2.2, 4.3 and 11 min, respectively. (C) Relative positions of the side chains are shown for each corresponding variant described in (B). The backbone has been omitted for clarity.

quenching was seen in the RF variant, with the addition of a phenylalanine at position 257. The changes in tryptophan emission among the variants suggested that the nature and proximity of residues 254 and 257 affected the emission of neighboring fluorophores and resulted in different spectral intensities for similarly folded enzymes. Because of the proximity of W302 to residues 254 and 257, these results further suggested that W302 might have some primary responsibility for the signal observed in the $N_2 \leftrightarrow I_2$ transition.

The binding of ANS to the enzyme was used to assess changes in the hydrophobic surface area. ANS emission was

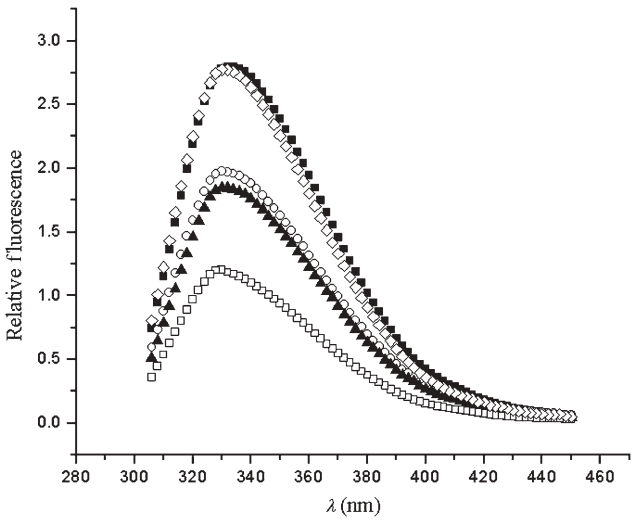

Fig. 5. Selective tryptophan fluorescence spectra of OPH enzymes. Protein concentrations were 100 μg/ml. The excitation wavelength was 295 nm and the fluorescence emission was recorded between 310 and 450 nm at 25°C. HH (◇), HL (■), RL (▲), RH (○), RF (□). The HH and HL enzymes have the greatest fluorescence emission. An arginine at position 254 results in quenching of fluorescence emission, as seen for the RL and RH enzymes. The combination of an arginine at position 254 and a phenylalanine at position 257 results in the greatest fluorescence quenching, as seen for the RF enzyme.

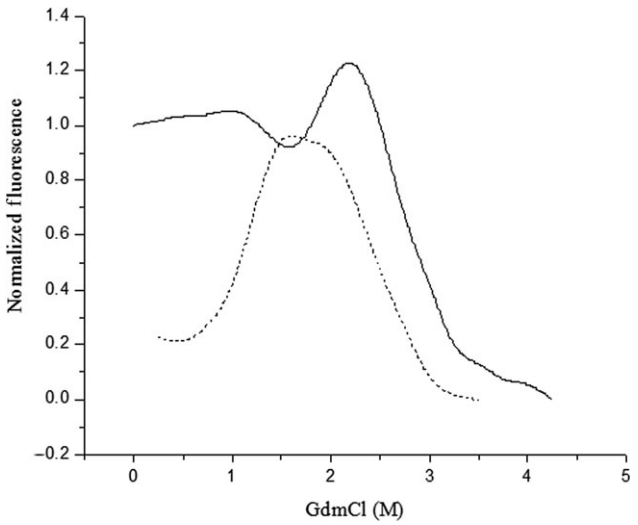

Fig. 6. Tryptophan fluorescence of ANS binding. Normalized fluorescence of the RH variant (solid line) and RH + 50 μM ANS (dashed line) at the corresponding GdmCl concentrations. Excitation and emission wavelengths for RH were 278 and 320 nm, respectively, while those for RH + ANS were 385 and 470 nm. The maximum in ANS fluorescence emission upon binding to RH corresponds to the local minimum in RH fluorescence between 1 and 2 M GdmCl. The RF profile, omitted for clarity, displays a similar local minimum in fluorescence at the same GdmCl concentration (Fig. 3) and corresponding maximum ANS emission.

observed to be maximal at a point that coincided with the minimum in the fluorescence emission between 1 and 2 M GdmCl in the RH and RF variants (Fig. 6). This suggested that the RH and RF variants had a solvent accessible hydrophobic region at these denaturant concentrations that is absent from other variants.

Rational design enhancement of V-type nerve agent hydrolysis

The activity of the native HH enzyme varies from rate limits with the P–O substrate paraoxon of 6900 s^{-1} to k_{cat} rates as low as 4 s^{-1} with the P–S substrate demeton-S, resulting in a 1725-fold range in activity among the various substrates (Table II). The HL variant activity was similar to that of the wild-type OPH with demeton-S, an analog for VX and VR. The RH variant showed increased activity with demeton-S nine times over that of the wild-type HH enzyme. The combination of the H254R and H257L substitutions in the RL variant resulted in demeton-S activity that was over 14 times that of the HH (Table II). Comparison of the kinetics of the hydrolysis of OP neurotoxins by the variant enzymes verified that RF exhibited the desired activity, with a k_{cat} of 34 $s^{-1}$for the P–S substrate demeton-S, the common V-agent surrogate. This was accompanied by a corresponding decrease in paraoxonase activity to a k_{cat} of 448 s^{-1} (Table II).

At 2 mM substrate with the V-agents, the RL variant was the most effective enzyme for the turnover of VX (144 s^{-1}) and VR (465 s^{-1}) (Table II). This is a 10X and 39X increase over the rates of the wild-type HH enzyme (14 and 12 s^{-1} for VX and VR, respectively). The RF variant had a kinetic profile that was intermediate to the HH and RL enzymes for these P–S bond V-agents, with rates of 68 and 36 s^{-1}, respectively. Unfortunately, concentration limitations established for research with surety materials at USAMRICD precluded substrate saturation studies. At concentrations of

Table II. Kinetic constants of OPH variants

Enzyme		Paraoxon			Demeton-S			VX	VR
		k_{cat} s^{-1}	K_M (mM)	k_{cat}/K_M^a	k_{cat} s^{-1}	K_M (mM)	k_{cat}/K_M^a	s^{-1b}	s^{-1b}
HH	H254, H257	6900	0.1 ± 0.05	6.90×10^7	3.5	4.4 ± 1.7	7.95×10^2	14	12
HL	H254, H257L	8000	0.3 ± 0.01	2.67×10^7	3.3	1.9 ± 0.9	1.74×10^3	ND[c]	ND[c]
RL	H254R, H257L	640	0.07 ± 0.01	9.14×10^6	50	6.2 ± 1.4	8.06×10^3	144	465
RH	H254R, H257	1200	0.09 ± 0.01	1.33×10^7	32	4.2 ± 1.0	7.62×10^3	ND[c]	ND[c]
RF	H254R, H257F	450	0.05 ± 0.02	9.00×10^6	34	7.6 ± 2.3	4.47×10^3	68	36

[a]M^{-1} s^{-1}
[b]μmol V-agent hydrolyzed/second/μmol enzyme at 2 mM V-agent.
[c]Not determined.

2 mM agent and below, the enzymes were not saturated, so it is not clear whether the increase in activity is a result of a change in the catalytic constant or substrate affinity.

Rational design increase in the global stability of OPH

The protein crystallized in space group C2, with unit cell dimensions $a = 128.80$ Å, $b = 90.60$ Å, $c = 69.14$ and $\beta = 91.74°$ (Table III). The bulky phenyl side chain of 257 makes a number of van der Waals contacts with hydrophobic residues in the substrate-binding pocket, increasing the hydrophobicity of the pocket, although reducing its size slightly (Fig. 7). This supports the hypothesis that the re-establishment of aromatic stacking and hydrophobic interactions in the vicinity of the active site has contributed to the stability of the RF variant.

A comparison of the cation–π interactions of three OPH enzymes is shown in Table IV. The RF variant has additional cation–π interactions compared with the H254R enzyme (PDB:1QW7). In addition to the significant contribution from the Arg254 and Phe257 interaction (3.88 *k*cal/mol), one additional contact appears to exist within the dimeric interface, contributing interaction energy of 3.12 *k*cal/mol. The total energy, E_{tot}, of the combined cation–π interactions, which include electrostatic and van der Waals contributions, in the RF enzyme was 10 *k*cal/mol. This indicated that cation–π interactions make a substantial contribution to the stability of RF.

Table III. Data collection and refinement statistics[a]

Data collection	
Space group	C2
Cell dimensions	
a, *b*, *c* (Å)	128.80, 90.60, 69.14
α, β, γ (°)	90, 91.74, 90
Resolution (Å)	50–2.15 (2.23–2.15)
R_{merge} (%)	6.0 (10.2)
$I/\sigma I$	55.2 (28.1)
Completeness (%)	94.0 (74.4)
Redundancy	3.8 (3.6)
Refinement	
Resolution (Å)	50–2.15
No. of reflections	40 319
R_{work}/R_{free}	18.8/21.8
No. of atoms	
Protein	5126
Ligand/ion	32/4
Water	463
B-factors	
Protein	26.3
Ligand/ion	35.4
Water	40.2
R.m.s. deviations	
Bond lengths (Å)	0.006
Bond angles (°)	1.31

[a]Data were collected from a single crystal. Values in parentheses are for the highest-resolution shell.

Discussion

OPH is capable of hydrolyzing a wide spectrum of OP compounds containing P–O, P–F, P–CN or P–S bonds, with different catalytic efficiencies. A comparison of the relative activities of 254 and 257 variant enzymes indicated that an arginine substitution at position 254 was important for the increases in activity with phosphonothioate (P–S) substrates. Analysis of specific catalytic activities with various OP substrates demonstrated that the RF variant exhibited the desired enhancement of activities against demeton-S, VX and VR (Table II). For other R variants, these relative activity enhancements have been reported to be associated with an enlargement of the active site, allowing it to accommodate the bulkier P–S substrates (diSioudi *et al.*,1999b). However, the active site is comprised of three distinct regions described as large, small and leaving group pockets (Chen-Goodspeed *et al.*, 2001a,b) and residue 257 is located at the boundary between the large pocket and the leaving group pocket. As

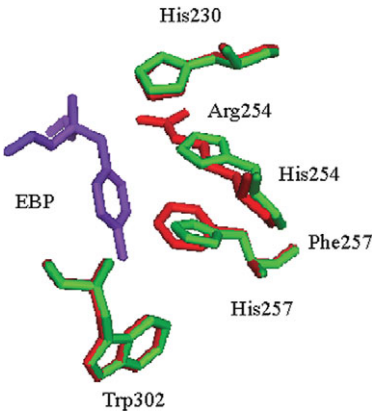

Fig. 7. The stacking network near the active site of the RF variant (red) overlaid with the wild-type structure (1DPM) (green). The purple stick figure is the substrate analog, EBP, which crystallized in the wild-type active site of 1DPM. The bulky phenylalanine residue reduces the size of the active site slightly, and appears to re-establish the stacking network lost in the RL and HL enzymes, both of which are less stable.

Table IV. Energetically significant cation–π interactions[a] (detected in the Structure of HH, RH and RF)

Structure	Amino acid		*E* (elec) (*k*cal/mol)	*E* (vdw) (*k*cal/mol)	E_{tot}
HH[b]	Arg141-A[c]	Trp69-B	−2.16	−0.77	−2.93
RH	Arg141-B	Trp69-A	−2.11	−0.83	−2.94
RF	Arg141-A	Trp69-B	−2.34	−0.81	−3.15
	Arg141-B	Trp69-A	−2.33	−0.79	−3.12
	Arg254-B	Phe257-B	−1.51	−2.37	−3.88
				RF Total	−10.15

[a]Cation–π interactions were analyzed using the program CaPTURE (Gallivan and Dougherty, 1999). Electrostatic (elec) and van der Waals (vdw) components of the calculated cation–π interaction energy are shown.
[b]HH (1DPM; Vanhooke *et al*., 1996); RH (1QW7;Grimsley *et al*., 2005); RF (this study).
[c]Capital letters associated with the residue number indicates the A or B chain of the OPH dimer.

might be expected with the insertion of the larger phenylalanine moiety at this position, the crystal structure revealed that the pocket size is actually decreased slightly as compared with the native HH enzyme. In spite of this, the activity with demeton-S is increased 10- and 5- fold with VX.

In order to balance the loss of an enzyme's stability with its gain in catalytic activity, substituting a phenylalanine at position 257 produced an enzyme, which preserved, and even enhanced, the stability of the HH. By inserting the positively charged arginine at position 254 and the phenylalanine at position 257, the planes of the aromatic rings of W302 and F257 are 4.00 Å from each other compared with 4.3 Å in the HH enzyme. The insertion of an aliphatic leucine at position 257 in the HL and RL variants would be expected to disrupt this interaction with W302 (Fig. 4C), and this disruption would be expected to have a significant effect on global stability. Although the RL variant was very effective at hydrolyzing P–S bonds, the increase in activity did coincide with a loss of thermodynamic stability (Table I).

The modifications of the more temperature-stable variants, RH and RF, appeared to have prevented localized unfolding, as evidenced by enhanced resistance to proteolysis. Thus, the phenylalanine of the RF variant provided more stability than the histidines of the HH and RH enzymes (Fig. 4B). In thermolysin digests at 65°C, the RH and RF variants had half-lives which are estimated to be 2–5 times longer than that of the wild-type enzyme. The stabilities determined from the thermolysin digests of RL, HL and the wild-type HH correlated with those seen in the chemical denaturation experiments and supported the interpretation that RH and RF are more stable proteins. This supported the hypothesis that the characteristics of the residue at position 257 play an important role in determining the stability of the enzyme. Variants with an aliphatic side chain at position 257 (RL and HL) were consistently the least stable, while those with an aromatic side chain were the most stable. Phenylalanine produced a significantly more stable enzyme than the less hydrophobic histidine (Fig. 4B). According to the crystal structure, the presence of a phenylalanine at position 257 introduces a cation–π interaction with Arg254, providing 3.88 *k*cal/mol to the overall global stability of RF (Table IV).

It is possible to construct a model for the initial unfolding of OPH around the active site. In this case, a local minimum in the fluorescence signal between 1 and 2 M GdmCl was coincident with a maximum in ANS binding, suggesting a rearrangement or compaction of the protein without a significant loss of structure at this point in the unfolding pathway. Those variants with an arginine at position 254 apparently have some hydrophobic surface that is accessible to ANS, yet not solvent exposed, and which is not present in the HH or HL variant. In combination, the fluorescence and ANS data support the hypothesis that 254R variants possess structure not present in the other enzymes and unfold via a more complex pathway. Structural changes similar to the HH and HL variants have been observed for other enzymes such as ribonuclease A and dihydrofolate reductase, in which the loss of activity upon exposure to denaturants preceded any detectable global change in the protein (Zou, 2001). The importance of position 257 to both the structural integrity of the enzyme and its catalytic activity highlights the relationship of structural flexibility and catalysis in this enzyme. While the contribution of the stacking interactions between residues 257 and 302 to stability is small, it occupies a location that is critical in determining the relative stability and substrate specificity of OPH. Cation–π interactions have been shown to provide an additional 7 *k*cal/mol to the stability of RF, with 3.88 *k*cal/mol contributed by the Arg254–Phe257 interaction (Table IV). The RL and HL variants, with an aliphatic leucine in place of the native histidine at position 257, displayed a decrease of 5–6 *k*cal/mol in thermodynamic stability compared with the native HH enzyme.

Small variations in stability greatly affect the concentration of protein in the native state near the apparent melting temperature because of the cooperative nature of folding. Thus, even modest increases in stability can result in large shifts among the conformational populations of a protein. For example, at 27°C both the HH and RL enzymes are over 99% in the folded form (data not shown). At 66°C the folded fractions are shifted to 28% for the RL and 80% for the HH. This observation emphasized the effect that small changes in stability can have on enzyme conformation, and coincidentally on activity. The balance of structural flexibility and catalytic characteristics can have significant implications in industrial applications, such as the disposal of CWAs, where increasing the reaction temperature by only a few degrees can greatly affect the speed of hydrolysis by enzymes stable at higher temperatures. The combination of hydrophobic and cation–π interactions near the active site of OPH are subject to such balancing. In this case, the increased hydrophobic interactions in the RF variant resulted in an enzyme that was more stable than the HH, yet retained the desirable catalytic characteristics with P–S substrates, including the nerve agents VX and VR. Using rational design and an understanding of side chain interactions, this study has shown that it is possible to increase the stability of a V-agent hydrolyzing enzyme while retaining the desired catalytic properties.

Funding

US Army Medical Research and Materiel Command [Cooperative Agreement #DAMD 17-00-2-0010]; the National Science Foundation [Grants MCB9904635 and CTS-0330189]. This work was also funded by the National Institutes of Health CounterACT Program through the National Institute of Neurological Disorders and Stroke (award #U01 NS058035-07). Its contents are solely the

responsibility of the authors and do not necessarily represent the official views of the federal government.

References

Adkins,S., Gan,K.N., Mody,M. and Ladu,B.N. (1991) *FASEB J.*, **5**, A483.

Arnold,U. and Ulbrich-Hofmann,R. (2001) *Eur. J. Biochem.*, **268**, 93–97.

Aubert,S.D., Li,Y.C. and Raushel,F.M. (2004) *Biochemistry*, **27**, 5707–5715.

Benning,M.M., Kuo,J.M., Raushel,F.M. and Holden,H.M. (1994) *Biochemistry*, **33**, 15001–15007.

Benning,M.M., Kuo,J.M., Raushel,F.M. and Holden,H.M. (1995) *Biochemistry*, **34**, 7973–7978.

Brunger,A.T., *et al*. (1998) *Acta Crystallogr. D Biol. Crystallogr.*, **54**, 905–921.

Chen-Goodspeed,M., Sogorb,M.A., Wu,F.Y., Hong,S.B. and Raushel,F.M. (2001a) *Biochemistry*, **40**, 1325–1331.

Chen-Goodspeed,M., Sogorb,M.A., Wu,F.Y. and Raushel,F.M. (2001b) *Biochemistry*, **40**, 1332–1339.

Cheng,T.C., Harvey,S.P. and Chen,G.L. (1996) *Appl. Environ. Microbiol.*, **62**, 1636–1641.

Dacre,J.C. (1984) In Brzin,M., Barnard,E.A. and Sket,D. (eds), *Cholinesterases, Fundamental and Applied Aspects*. de Gruyter, Berlin, p. 415.

diSioudi,B.D., Miller,C.E., Lai,K., Grimsley,J.K. and Wild,J.R. (1999a) *Chem Biol Interact*, **119–120**, 211–223 [Review, 57 refs].

diSioudi,B.D., Grimsley,J.K., Lai,K. and Wild,J.R. (1999b) *Biochemistry*, **38**, 2866–2872.

Gallivan,J.P. and Dougherty,D.A. (1999) *Proc. Natl Acad. Sci.*, **96**, 9459–9464.

Gallo,B.J. and Lawryk,N.J. (1991) In Hayes,W.J. and Laws,E.R. (eds), *Handbook of Pesticide toxicology, Vol. 2; Classes of Pesticides*. Academic Press, Inc., San Diego, CA, pp. 917–983.

Garden,J.M., Hause,S.K., Hoskin,F.C.G. and Roush,A.H. (1975) *Comp. Biochem. Physiol. C Pharmacol. Toxicol. Endocrinol.*, **52**, 95–98.

Grimsley,J.K., Scholtz,J.M., Pace,C.N. and Wild,J.R. (1997) *Biochemistry*, **36**, 14366–14374.

Grimsley,J.K., Calamini,B., Wild,J.R. and Mesecar,A.D. (2005) *Arch. Biochem. Biophys.*, **442**, 169–179.

Grognet,J.M., Ardouin,T., Istin,M., Vandais,A., Noel,J.P., Rima,G., Satge,J., Pradel,C., Sentenac-Roumanou,H. and Lion,C. (1993) *Arch. Toxicol.*, **67**, 66–71.

Hill,C.M., Li,W.S., Thoden,J.B., Holden,H.M. and Raushel,F.M. (2003) *J. Am. Chem. Soc.*, **125**, 8990–8991.

Hong,S.B. and Raushel,F.M. (2004) *Protein Eng.*, **388**, 256–266.

Jones,T.A. and Kjeldgaard,M. (1997) *Methods Enzymol. 277*. Academic Press, 173–230.

Kolakowski,J.E., Defrank,J.J., Harvey,S.P., Szafraniec,L.L., lBeaudry,W.T., Lai Kaihua and Wild,J.R. (1997) *Biocatal. Biotransform.*, **15**, 297–312.

Lai,K., Stolowich,N.J. and Wild,J.R. (1995) *Archives of Biochem. Biophys.*, **318**, 59–64.

Lai,K.H., Grimsley,J.K., Kuhlmann,B.D., Scapozza,L., Harvey,S.P., DeFrank,J.J., Kolakowski,J.E. and Wild,J.R. (1996) *Chimia*, **50**, 430–431.

Lewis,V.E., Donarski,W.J., Wild,J.R. and Raushel,F.M. (1988) *Biochemistry*, **27**, 1591–1597.

Masson,P., Josse,D., Lockridge,O., Viguie,N., Taupin,C. and Buhler,C. (1998) *J. Physiol. Paris*, **92**, 357–362 [Review, 30 refs].

Mazur,A. (1947) *J. Biol. Chem.*, **164**, 271–289.

McDaniel,C.S., Harper,L.L. and Wild,J.R. (1988) *J. Bacteriol.*, **170**, 2306–2311.

McPherson,A. (1999) *Crystallization of Biological Molecules*. Cold Spring Harbor Laboratory Press, Cold Spring Harbor, NY, pp. 188–192.

Millard,C.B., Lockridge,O. and Broomfield,C.A. (1998) *Biochemistry*, **37**, 237–247.

Mulbry,W.W., Karns,J.S., Kearney,P.C., Nelson,J.O., McDaniel,C.S. and Wild,J.R. (1986) *Appl. Environ. Microbiol.*, **51**, 926–930.

Otwinowsky,Z. and Minor,W. (1997) *Methods Enzymol. 276: Macromolecular Crystallography, part A*. Academic Press, pp. 307–326.

Pace,C.N. and Scholtz,J.M. (1997) In Creighton,T.E. (ed.), *Protein Structure: A Practical Approach*, 2nd edn. Oxford University Press, pp. 299–321.

Rastogi,V.K., DeFrank,J.J., Cheng,T.C. and Wild,J.R. (1997) *Biochem. Biophys. Res. Commun.*, **241**, 294–296.

Roodveldt,C. and Tawfik,D.S. (2005) *Protein Eng Des Sel*, **18**, 51–58.

Vanhooke,J.L., Benning,M.M., Raushel,F.M. and Holden,H.M. (1996) *Biochemistry*, **35**, 6020–6025.

Yang,H., Carr,P.D., McLoughlin,S.Y., Liu,J.W., Horne,I., Qiu,X., Jeffries,C.M.J., Russell,R.J., Oakeshott,J.G. and Ollis,D.L. (2003) *Protein Eng.*, **16**, 135–145.

Yx,C., Yx,Z., Guo,Z.Q., Rong,K.T. and Chang,W.B. (1995) *Arch. Toxicol.*, **69**, 565–567.

Zou,C.L. (2001) *Shen Li Ke. Xue. Jin. Zhan.*, **32**, 7–12.

Received July 17, 2007; revised March 9, 2008; accepted March 18, 2008

Edited by Rick Wierenga